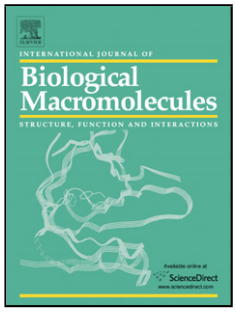

Title: Hydration-induced crystalline transformation of starch polymer under ambient conditions

Authors: Dongling Qiao, Binjia Zhang, Jing Huang, Fengwei Xie, David K. Wang, Fatang Jiang, Siming Zhao, Jie Zhu

PII: S0141-8130(17)30467-1
DOI: http://dx.doi.org/doi:10.1016/j.ijbiomac.2017.05.008
Reference: BIOMAC 7495

To appear in: *International Journal of Biological Macromolecules*

Received date: 6-2-2017
Revised date: 30-4-2017
Accepted date: 2-5-2017

Please cite this article as: Dongling Qiao, Binjia Zhang, Jing Huang, Fengwei Xie, David K.Wang, Fatang Jiang, Siming Zhao, Jie Zhu, Hydration-induced crystalline transformation of starch polymer under ambient conditions, International Journal of Biological Macromoleculeshttp://dx.doi.org/10.1016/j.ijbiomac.2017.05.008

Hydration-induced crystalline transformation of starch polymer under ambient conditions

Dongling Qiao[a], Binjia Zhang[b,*], Jing Huang[c], Fengwei Xie[d,**], David K. Wang[d], Fatang Jiang[a], Siming Zhao[b], Jie Zhu[e]

[a] *Glyn O. Philips Hydrocolloid Research Centre at HUT, Hubei University of Technology, Wuhan 430068, China*

[b] *Key Laboratory of Environment Correlative Dietology (Ministry of Education), College of Food Science and Technology, Huazhong Agricultural University, Wuhan 430070, China*

[c] *Hubei Light Industry Technology Institute, Wuhan 430070, China*

[d] *School of Chemical Engineering, The University of Queensland, Brisbane, Qld 4072, Australia*

[e]*School of Chemical Engineering and Energy Technology, Dongguan University of Technology, Dongguan 523808, China*

[*] Corresponding Author. Email: zhangbj@mail.hzau.edu.cn (B. Zhang)

[**] Corresponding Author. Email: f.xie@uq.edu.au, fwhsieh@gmail.com (F. Xie)

Graphical abstract

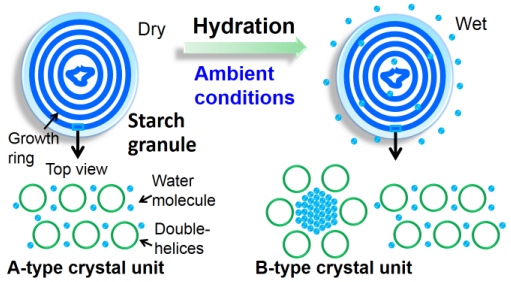

Highlights:

- Starch under hydration at ambient conditions was studied by synchrotron SAXS/WAXS
- Hydration transformed some A-type starch crystallites into B-type forms
- Hydration enhanced the B-polymorphic features for both A-type and B-type starches

Abstract: With synchrotron small/wide-angle X-ray scattering (SAXS/WAXS), we revealed that post-harvest hydration at ambient conditions can further alter the starch crystalline structure. The hydration process induced the alignment of starch helices into crystalline lamellae, irrespective of the starch type (A- or B-). In this process, non-crystalline helices were probably packed with water molecules to form new crystal units, thereby enhancing the overall concentration of starch crystallinity. In particular, a fraction of the monoclinic crystal units of the A-type starches encapsulated water molecules during hydration, leading to the outward movement of starch helices. Such movement resulted in the transformation of monoclinic units into hexagonal units, which was associated with the B-type crystallites. Hence, the hydration under ambient conditions could enhance the B-polymorphic features for both A-type and B-type starches. The new knowledge obtained here may guide the design of biopolymer-based liquid crystal materials with controlled lattice regularity and demanded features.

Keywords: *Hydration; starch; crystalline structure; crystals; crystallinity*

Abbreviations:

WMS, waxy maize starch; RMS, regular maize starch; GMS, Gelose 50 high-amylose maize starch; PS, potato starch; SAXS, small-angle X-ray scattering; WAXS, wide-angle X-ray scattering

1 Introduction

Nanopattern with controlled regularity has an enormous advantage in designing anisotropic materials because of their broad utility and versatility in optics [1], electronics [2, 3], and bioengineering [4]. Liquid crystals, as anisotropic mesophases existing between solid crystal and isotropic liquid, have attracted increasing attention [2]. The molecules with liquid crystal behaviors, *viz.*, mesogens, are generally organized into regular nanoscale units (*i.e.*, lattices) via non-covalent forces (*e.g.*, hydrogen bonding) [5]. The functionalities (optical, electronic and sensing properties [1, 2, 5]) of liquid crystals highly depend on the shape and size of the lattices. Hence, manipulating the lattice pattern of liquid crystals stands at the core of tailoring their performance. For controlling the morphology of liquid crystal cells, mesogens with different sizes and shapes have been reported, including the smectic, columnar, cubic and discotic forms [6] originated from metal, ionic and polymeric materials [2]. However, the development of liquid crystals using these mesogens requires tedious multi-step reactions and purification processes, as well as severe experimental conditions.

In contrast, natural polymers such as cellulose and starch provide fascinating models for creating nano-materials with precisely controlled dimensions [7-10]. These polymers are not only widely available and sustainable but also biodegradable and biocompatible, and thus have several economic and environmental advantages. Starch is a typical natural polymer with the liquid crystal property [11], and it includes two major glucan polymers, *i.e.*, amylose and amylopectin [12, 13]. These two biopolymers form crystalline and amorphous areas in the native starch granule to construct a multi-level semicrystalline structure [14-16]. In particular, the double

helices of starch chains exist as mesogens [11] and are also the key structural units in the starch granule. The organization of the starch helices within the nanoscale crystal cells governs the crystalline structure of starch. There are mainly two types of crystalline structures of starch including A-type with monoclinic crystal cells and B-type with hexagonal crystal units [17]. The understanding of how the external conditions influence the organization of starch helices into the different crystal cells could open research avenues into artificially designing liquid crystals with regular nanoscale patterns.

The organization of post-harvest starch helices into either the A- or B-type crystal cell closely relates to the amount of water molecules. While A-type starch crystallites contain only eight inter-helical water molecules in each monoclinic crystal unit with tightly packed helices, the B-type crystallites have 36 water molecules in each hexagonal crystal unit with a more open packing of helices [17]. The cereal starches (*e.g.*, wheat, rice) normally contain A-type crystallites, whereas tuber, fruit and stem starches (*e.g.*, potato, banana) often have B-type crystallites. Nonetheless, the mechanism on how the growth of plants relates to the starch crystalline type, *i.e.*, the manner of helices organized into the crystal cells, is still not fully understood. Moreover, besides the cultivar, the thermal processing of starch with water, *e.g.*, extruding and compression molding, also tends to change starch crystalline structure [18, 19]. This change might result from the disruption of original crystallites and the realignment of helices into the crystal cells to form new crystallites with the same or an altered type. However, while in these cases a combination of multiple conditions (such as temperature, moisture, and so forth) with complex variation patterns are involved, it is challenging to derive general bionic inspirations for the design of liquid

crystals where artificial (*e.g.*, post-harvest) and spontaneous (*e.g.*, at ambient conditions) processes are preferred.

Considering the crucial role of water molecules in constructing starch crystal cells, here we test whether the hydration alone under ambient conditions can spontaneously alter the manner of the starch helical organization into crystal cells, *i.e.*, the type of starch crystallites. If so, the related evolution in the assembly of starch helices (mesogens) within the crystal units would provide valuable information for the rational and simple development of natural, starch-based liquid crystals with regulated nanoscale morphology and thus demanded performance. Though earlier findings show that hydration might increase the starch crystallinity [20, 21], it is unaccounted for whether post-harvest hydration can induce any changes in the crystalline type. To this end, we evaluated the effects of hydration under ambient conditions (*ca.* 26 °C) on the crystalline structure of four starches using synchrotron SAXS/WAXS techniques. Based on the results, we discussed the underlying mechanism regarding how hydration changes the starch crystalline features.

2 Materials and methods

2.1 Materials

Waxy maize starch (WMS), regular maize starch (RMS), and Gelose 50 maize starch (GMS) were supplied by Penford Australia Ltd. (Lane Cove, NSW Australia). WMS, RMS, and GMS had amylose contents of *ca.* 3%, 24% and 56%, respectively, as measured using an iodine colorimetric method [22]. Potato starch (PS) with an amylose content of *ca.* 36% was purchased from Avebe (Netherlands). A moisture

analyzer (MA35, Sartorius Stedim Biotech GmbH, Germany) was used to measure the moisture content (MC) of starch. The MC for the maize starches was *ca*. 13%, while that for PS was *ca*. 14%.

2.2 Small/wide angle X-ray scattering (SAXS/WAXS)

SAXS/WAXS measurements with 1 s acquisition were carried out on the SAXS/WAXS beamline (flux, 10^{13} photons/s) installed at the Australian Synchrotron (Clayton, Australia) [23], at a wavelength λ = 1.54 Å. The 2D scattering patterns were recorded using a Pilatus 1M camera (active area 169 × 179 mm and pixel size 172 × 172 μm) and a Pilatus 200K camera (active area 169 × 33 mm and pixel size 172 × 172 μm). The 1D data were acquired from the 2D scattering patterns using the Scatterbrain software. The starch powders without adding any water were used as the dry (*i.e.*, non-hydrated) starch samples. Also, to fully hydrate those four starches, the starch slurries containing 40% starch were prepared in vials with careful blending, and then kept under ambient conditions (*i.e.*, 26 °C) for 1 h. The resulted starch slurries were used as the hydrated starch samples. Both non-hydrated and hydrated starches were tested. The scattering of a Kapton tape (5413 AMBER 3/4IN X 36YD, 3M, USA) on the stage window was used as the background for the starches before hydration, and the scattering of pure water with the Kapton tape was used as the background for the hydrated starches. All data were collected at 26 °C and were background subtracted and normalized. Each test was conducted in triplicate to obtain reliable scattering results.

The configuration covered $0.015 < q < 2.9$ Å^{-1} simultaneously by establishing a slight overlap in q (see **Fig. S1** in Support Information). The scattering vector, q, was defined as $q = 4\pi\sin\theta/\lambda$, in which 2θ is the scattering angle and λ is the wavelength of the X-ray source. The data in the range of $0.015 < q < 0.20$ Å^{-1} were used as the SAXS patterns. The data in the range of $0.28 < q < 2.8$ Å^{-1} (*ca.* $4° < 2\theta$ for Cu Kα < 40°) were used as the WAXS patterns. The relative crystallinity (X_c, %) of starch was calculated using the PeakFit software (Ver. 4.12) [24], according to Eq. (1):

$$X_c = \frac{\sum_{i=1}^{n} A_{ci}}{A_t} \qquad (1)$$

where A_{ci} is the area under each crystalline peak with the index i, and A_t is the total area of the WAXS pattern.

2.3 Statistical analysis

Data were expressed as means ± standard deviations, and were analyzed by the one-way ANOVA and multiple comparison tests with a least significant difference using the IBM SPSS software version 20.0 (Chicago, IL, USA). A statistical difference of $P < 0.05$ was considered significant.

3 Results and discussion

3.1 Synchrotron SAXS analysis

Fig. 1 shows the double-logarithmic and Lorentz-corrected synchrotron SAXS patterns of WMS, RMS, GMS, and PS before hydration. Dry RMS displayed a modest peak at *ca.* 0.07 $Å^{-1}$ (q_{peak1} for dry samples) (see **Table 1** and **Fig. 1A**), ascribed to the semi-crystalline lamellar structure of starch [25, 26]. Also, dry RMS featured a second less-resolved peak at *ca.* 0.15 $Å^{-1}$ (q_{peak2} for dry samples), which was probably the second order reflection of the lamellar arrangement [21]. Dry WMS and dry PS had a lamellar peak at *ca.* 0.09 $Å^{-1}$ and 0.08 $Å^{-1}$ respectively, though the peak has never been detected by the bench-scale SAXS instrument for dry PS. From the Lorentz-corrected SAXS patterns in **Fig. 1B**, a very weak peak at *ca.* 0.08 $Å^{-1}$ was seen for dry GMS powder. All these results indicate that, before hydration, only a small part of starch helices could be aligned into the crystalline lamellae to construct the semi-crystalline lamellar structure.

Fig. 2 shows the Lorentz-corrected SAXS patterns of WMS, RMS, GMS, and PS after hydration in excess water at room temperature. All starches produced a strong lamellar peak at 0.06 to 0.07 $Å^{-1}$ (q_{peak1} for wet samples in **Table 1**), while the SAXS profiles of WMS and RMS displayed a less-resolved peak at *ca.* 0.13 $Å^{-1}$ (q_{peak2} for wet samples in **Table 1**). This result suggests that, after hydration, the starches changed from a glassy nematic state to a smectic state [27], due to liquid crystal nature of the side-chains of these starches [18]. In this case, an increased amount of starch helices were aligned into the crystalline lamellae, which enhanced the intensity of the scattering peak for the lamellar structure. Since starch helices are typically packed into the crystal unit cells to form starch crystallites, the evolutions in

the alignment of starch helices during hydration might alter the crystalline type of starch. In order to further understand this conjecture, we interrogated the potential changes in starch crystalline structure by employing WAXS technique.

3.2 Synchrotron WAXS analysis

The type of crystalline structure of starch can be accurately distinguished by inspecting the WAXS patterns. **Fig. 3** shows the synchrotron WAXS patterns of WMS, RMS, GMS and PS before (**Fig. 3A**) and after (**Fig. 3B**) hydration. The WAXS scattering profiles of the dry GMS and PS show the B-type crystalline structure with the strongest peak at *ca.* 1.21 $Å^{-1}$, several smaller peaks at *ca.* 1.07, 1.56 and 1.70 $Å^{-1}$, and a characteristic peak at *ca.* 0.40 $Å^{-1}$. On the other hand, the dry WMS and RMS show the A-type crystalline structure with intense peaks at *ca.* 1.07 and 1.63 $Å^{-1}$ and an unresolved doublet at *ca.* 1.21 and 1.28 $Å^{-1}$. After hydration, the corresponding dominant crystalline type of each of the starches was kept constant (*cf.* **Fig. 3B**).

As seen in **Table 1,** the relative crystallinity (X_c) values for the starches under dry and wet states are presented. It is observed that the hydrated starches had a larger X_c than did their dry starch counterparts. This result suggests that, during hydration, a proportion of non-crystalline starch helices organized into crystal cells with the water molecules via hydrogen bonds, which led to an increased quantity of the starch crystallites. Previous studies confirmed similar information that the increased moisture content contributed to the growing crystallinity of starch [28, 29].

Then, we further used the 100 inter-helix reflection for the B-type crystallites [21, 25], *i.e.*, the peak at *ca.* 0.40 $Å^{-1}$, to probe whether hydration partially alters starch crystalline type. **Fig. 4** shows the enlarged WAXS patterns in the range of $0.028 < q < 0.5$ $Å^{-1}$. As expected, dry GMS and PS had a characteristic peak at *ca.* 0.40 $Å^{-1}$; dry WMS and RMS exhibited an extremely weak inflection at *ca.* 0.40 $Å^{-1}$. **Table 1** lists the area ratio (R_{100}) of the 100 reflection peak over the whole WAXS pattern. The R_{100} values for dry GMS and PS were 1.80% and 2.68%, respectively, and this ratio was only between 0.02% and 0.03% for the dry WMS and RMS. This observation confirms that the dry A-type starches contained a minute amount to almost no B-type crystallites. However, in **Fig. 4**, while the hydrated GMS and PS had a stronger 100 inter-helix reflection than did their dry counterparts; the hydrated WMS and RMS showed a clearly-visible 100 inter-helix reflection. As a result, hydration of starches increased the value of R_{100} for all starches. In particular, WMS had a greater increase in R_{100} than that of the RMS (*cf*. **Table 1**). All these results clearly confirm that the hydration under ambient conditions (26 °C) transformed part of A-type starch crystallites into the B-type forms, *i.e.*, a transformation of the monoclinic crystal cells into the hexagonal crystal units.

3.3 Proposed mechanism of how hydration alters starch crystalline type

In different types of starch crystallites, their helices (*i.e.*, mesogens) interact differently with water molecules. Both A- and B-type starch crystallites are left-handed six-fold structures. Specifically, A-type crystallites are constructed by H-bonded parallel-stranded helices, *i.e.*, one double helices at the corner and another at

the center of the crystal unit cell (*cf*. **Fig. 5**), packed in a B2-monoclinic space group [15]. Such close-packed helices allow for only four water molecules in the inner of the unit cell (and for totally eight water molecules per unit). Water molecules thus cannot be removed from the monoclinic crystal cells of A-type starch unless a complete disruption of its crystalline structure takes place. In contrast, the helices of B-type crystallites are packed into a hexagonal unit cell (*cf*. **Fig. 5**), $P6_1$ space group [15]. The arrangement is more open and thus a larger number of water molecules can be located in a central channel surrounded by six double helices. Normally, thirty-six water molecules exist in the unit cell between the six double helices [17], forming a "column" of water surrounded by the hexagonal network.

Based on these facts, we propose that the availability of excess water molecules during plant growth governs the crystalline type of starch. Under humid growth environment, starches from tubers, stems, and fruits (*e.g.*, PS) normally have a B-type crystalline structure [17], whereas cereal starches from relatively dry environment (*e.g.*, WMS, RMS) contain mainly an A-type crystalline structure [26, 30]. Further attesting to this notion, for high-amylose starches with genetic modification (*e.g.*, GMS), the biosynthesis of amylopectin is greatly inhibited during crop growth, which reduces the amount of starch double-helices. Thus, the ratio of environmental water molecules to the double-helices is increased, which results in a production of high-amylose starches with dominantly a B-type crystalline structure [26].

During the post-harvest hydration, the available water molecules have the potential to plasticize the starch molecules within the branch points to maximize the entropy of starch backbone and increase its flexibility [21]. This follows the decoupling of the double-helices from the backbone and re-assemble into the

crystalline lamellae; yet the branch points pack into the amorphous lamellae (see **Fig. 5**). As a consequence, the proportion of semi-crystalline lamellae in the hydrated starches increased [11], leading to an increase in the visibility of lamellar peak as demonstrated in our study. Regardless of the original crystalline type of starch, part of non-crystalline helices in the dry starches encapsulated water molecules during hydration and thus formed crystal cells in the hydrated starches (*i.e.*, an increase in X_c).

In particular, a fraction of monoclinic crystal units of the A-type starches (WMS and RMS) trapped water molecules during hydration. This induced the outward movement of starch double-helices within the crystal units (see **Fig. 5**), which resulted in the formation of hexagonal crystal units with a central water channel (shown by the emergence of 100 reflection for hydrated WMS and RMS). Again, relative to RMS, WMS had more amylopectin and a larger quantity of double-helices. The double-helices in WMS suffered very weak constraint from amylose chains, as it only contained a very small amount of amylose. This enhanced the movement of WMS double-helices during hydration to form more hexagonal crystal units.

4 Conclusions

In summary, the effects of hydration under ambient conditions on the crystalline features of WMS and RMS with an A-type crystalline structure and GMS and PS with a B-type structure were investigated by synchrotron SAXS/WAXS techniques. We found that for both A- and B-type starches, not only could the helices be aligned into the crystalline lamellae with hydration, but also part of non-crystalline helices were

able to organize with water molecules to form new crystallites. In particular, for the A-type starches, a proportion of monoclinic crystal units could encapsulate water molecules during the hydration process. This trapping of water led to the outward movement of starch helices, and thus the formation of the hexagonal crystal units, *i.e.*, B-type crystallites. Therefore, hydration enhanced the B-crystalline features for both the A- and B-type starches under ambient conditions. Also, it is worth mentioning that more investigations, *e.g.*, the effects of water content and temperature and the in-depth understanding of crystal evolution, are underway to enhance the effectiveness of hydration at altering the crystalline type of starch polymer, in order to provide value-added inspirations for designing liquid crystals. Another important implication regarding the liquid crystal nature of starch is that these findings open the opportunity for the development of natural polymer-based liquid crystals that are responsive to simple hydration at room temperature without any energy input.

Acknowledgments

The authors would like to acknowledge the Doctoral Startup Foundation from Hubei University of Technology (BSQD2016024), the National Natural Science Foundation of China (31401586), the Fundamental Research Funds for the Central Universities (2662016QD008), the Hubei Provincial Natural Science Foundation of China (2016CFB142), and the Open Project Program of Provincial Key Laboratory of Green Processing Technology and Product Safety of Natural Products (201602). This research was undertaken on the SAXS/WAXS beamline at the Australian Synchrotron, Victoria, Australia.

References

[1] T. Woehrle, I. Wurzbach, J. Kirres, A. Kostidou, N. Kapernaum, J. Litterscheidt, J.C. Haenle, P. Staffeld, A. Baro, F. Giesselmann, S. Laschat, Discotic Liquid Crystals, Chem. Rev., 116 (2016) 1139-1241.

[2] K. Goossens, K. Lava, C.W. Bielawski, K. Binnemans, Ionic Liquid Crystals: Versatile Materials, Chem. Rev., 116 (2016) 4643-4807.

[3] X.J. Zhang, J.S. Jie, W. Deng, Q.X. Shang, J.C. Wang, H. Wang, X.F. Chen, X.H. Zhang, Alignment and Patterning of Ordered Small-Molecule Organic Semiconductor Micro-/Nanocrystals for Device Applications, Adv. Mater., 28 (2016) 2475-2503.

[4] L.J. Xue, J.L. Zhang, Y.C. Han, Phase separation induced ordered patterns in thin polymer blend films, Prog. Polym. Sci., 37 (2012) 564-594.

[5] Z. Hussain, F. Qazi, M.I. Ahmed, A. Usman, A. Riaz, A.D. Abbasi, Liquid crystals based sensing platform-technological aspects, Biosens. Bioelectron., 85 (2016) 110-127.

[6] C. Tschierske, Non-Conventional Liquid Crystals—the Importance of Micro-Segregation for Self-Organisation, J. Mater. Chem., 8 (1998) 1485-1508.

[7] M. Parvinzadeh Gashti, M. Stir, M. Bourquin, J. Hulliger, Mineralization of Calcium Phosphate Crystals in Starch Template Inducing a Brushite Kidney Stone Biomimetic Composite, Crystal Growth & Design, 13 (2013) 2166-2173.

[8] X. Pang, Y. He, J. Jung, Z. Lin, 1D nanocrystals with precisely controlled dimensions, compositions, and architectures, Science, 353 (2016) 1268-1272.

[9] D. Mumalo-Djokic, W.B. Stern, A. Taubert, Zinc Oxide/Carbohydrate Hybrid Materials via Mineralization of Starch and Cellulose in the Strongly Hydrated Ionic Liquid Tetrabutylammonium Hydroxide, Crystal Growth & Design, 8 (2008) 330-335.

[10] J. Xiang, H. Cao, J.H. Warner, A.A.R. Watt, Crystallization and Self-Assembly of Calcium Carbonate Architectures, Crystal Growth & Design, 8 (2008) 4583-4588.

[11] D.R. Daniels, A.M. Donald, Soft material characterization of the lamellar properties of starch: Smectic side-chain liquid-crystalline polymeric approach, Macromolecules, 37 (2004) 1312-1318.

[12] Q.Q. Jiang, W.Y. Gao, X. Li, J.Z. Zhang, Characteristics of native and enzymatically hydrolyzed Zea mays L., Fritillaria ussuriensis Maxim. and Dioscorea opposita Thunb. starches, Food Hydrocolloid, 25 (2011) 521-528.

[13] W.C. Liu, P.J. Halley, R.G. Gilbert, Mechanism of Degradation of Starch, a Highly Branched Polymer, during Extrusion, Macromolecules, 43 (2010) 2855-2864.

[14] K. Luengwilai, D.M. Beckles, Structural investigations and morphology of tomato fruit starch, J. Agric. Food Chem., 57 (2009) 282-291.

[15] A. Buléon, P. Colonna, V. Planchot, S. Ball, Starch granules: structure and biosynthesis, Int J Biol Macromol, 23 (1998) 85-112.

[16] S. Perez, E. Bertoft, The molecular structures of starch components and their contribution to the architecture of starch granules: A comprehensive review, Starch/Stärke, 62 (2010) 389-420.

[17] B. Zhang, S. Xiong, X. Li, L. Li, F. Xie, L. Chen, Effect of oxygen glow plasma on supramolecular and molecular structures of starch and related mechanism, Food Hydrocolloid, 37 (2014) 69-76.

[18] R. Vermeylen, V. Derycke, J.A. Delcour, B. Goderis, H. Reynaers, M.H. Koch, Gelatinization of starch in excess water: beyond the melting of lamellar crystallites. A combined wide- and small-angle X-ray scattering study, Biomacromolecules, 7 (2006) 2624-2630.

[19] H.S. Liu, F.W. Xie, L. Yu, L. Chen, L. Li, Thermal processing of starch-based polymers, Prog. Polym. Sci., 34 (2009) 1348-1368.

[20] A. Lopez-Rubio, B.M. Flanagan, A.K. Shrestha, M.J. Gidley, E.P. Gilbert, Molecular rearrangement of starch during in vitro digestion: toward a better understanding of enzyme resistant starch formation in processed starches, Biomacromolecules, 9 (2008) 1951-1958.

[21] J. Blazek, E.P. Gilbert, Effect of Enzymatic Hydrolysis on Native Starch Granule Structure, Biomacromolecules, 11 (2010) 3275-3289.

[22] I. Tan, B.M. Flanagan, P.J. Halley, A.K. Whittaker, M.J. Gidley, A method for estimating the nature and relative proportions of amorphous, single, and double-helical components in starch granules by C-13 CP/MAS NMR, Biomacromolecules, 8 (2007) 885-891.

[23] B. Zhang, F. Xie, T. Zhang, L. Chen, X. Li, R.W. Truss, P.J. Halley, J.L. Shamshina, T. McNally, R.D. Rogers, Different characteristic effects of ageing on starch-based films plasticised by 1-ethyl-3-methylimidazolium acetate and by glycerol, Carbohydr. Polym., 146 (2016) 67-79.

[24] A. Lopez-Rubio, B.M. Flanagan, E.P. Gilbert, M.J. Gidley, A novel approach for calculating starch crystallinity and its correlation with double helix content: a combined XRD and NMR study, Biopolymers, 89 (2008) 761-768.

[25] J. Doutch, E.P. Gilbert, Characterisation of large scale structures in starch granules via small-angle neutron and X-ray scattering, Carbohydr. Polym., 91 (2013) 444-451.

[26] B. Zhang, Y. Zhao, X. Li, L. Li, F. Xie, L. Chen, Supramolecular structural changes of waxy and high-amylose cornstarches heated in abundant water, Food Hydrocolloid, 35 (2014) 700-709.

[27] A. Lopez-Rubio, A. Htoon, E.P. Gilbert, Influence of extrusion and digestion on the nanostructure of high-amylose maize starch, Biomacromolecules, 8 (2007) 1564-1572.

[28] T.Y. Bogracheva, Y.L. Wang, C.L. Hedley, The effect of water content on the ordered/disordered structures in starches, Biopolymers, 58 (2001) 247-259.

[29] T.Y. Bogracheva, Y.L. Wang, T.L. Wang, C.L. Hedley, Structural studies of starches with different water contents, Biopolymers, 64 (2002) 268-281.

[30] D. Qiao, F. Xie, B. Zhang, W. Zou, S. Zhao, M. Niu, R. Lv, Q. Cheng, F. Jiang, J. Zhu, A further understanding of the multi-scale supramolecular structure and digestion rate of waxy starch, Food Hydrocolloid, 65 (2017) 24-34.

Figure Captions

Fig. 1 Double-logarithmic synchrotron SAXS patterns (A) and Lorentz-corrected synchrotron SAXS patterns (B) of dry waxy maize starch (WMS), regular maize starch (RMS), Gelose 50 high amylose maize starch (GMS), and potato starch (PS) before hydration under ambient conditions (26 °C).

Fig. 2 Lorentz-corrected SAXS patterns of waxy maize starch (WMS), regular maize starch (RMS), Gelose 50 high amylose maize starch (GMS) and potato starch (PS) after hydration under ambient conditions (26 °C).

Fig. 3 WAXS patterns ($0.028 < q < 2.8$ Å^{-1}, *ca.* $4 < 2\theta$ for Cu Kα < 40 °) of waxy maize starch (WMS), regular maize starch (RMS), Gelose 50 high amylose maize starch (GMS), and potato starch (PS) before (A) and after (B) hydration under ambient conditions (26 °C).

Fig. 4 Enlarged 100 inter-helix reflection peak at *ca.* 0.40 Å^{-1} of waxy maize starch (WMS), regular maize starch (RMS), Gelose 50 high amylose maize starch (GMS), and potato starch (PS) before (A) and after (B) hydration under ambient conditions (26 °C).

Fig. 5 Schematic mechanism for how hydration transforms part of A-type starch crystallites into the B-type forms under ambient conditions.

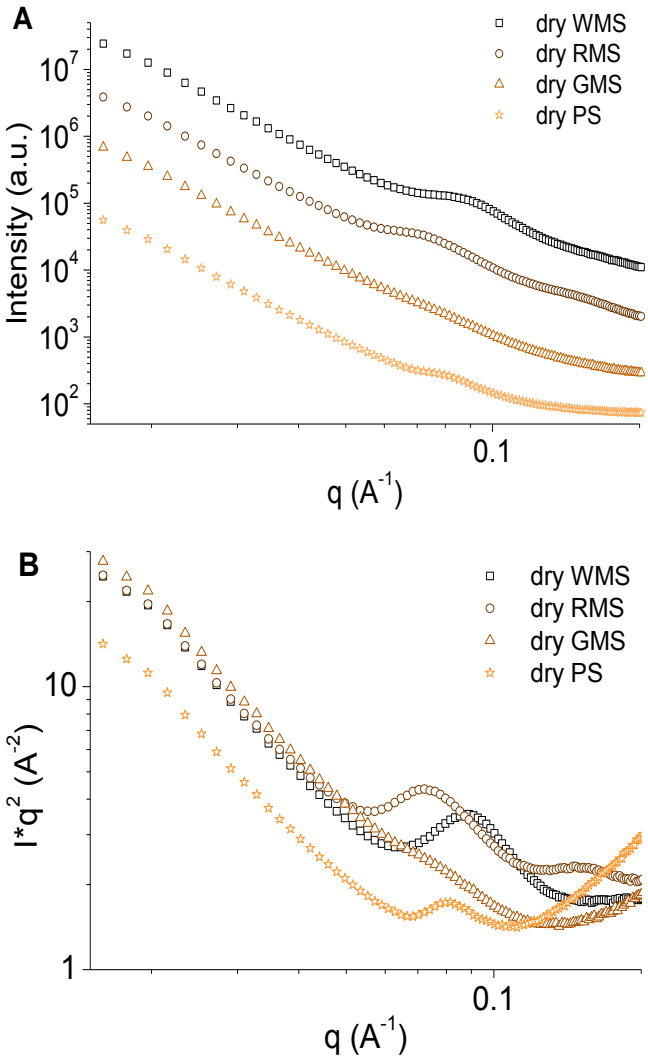

Fig. 1

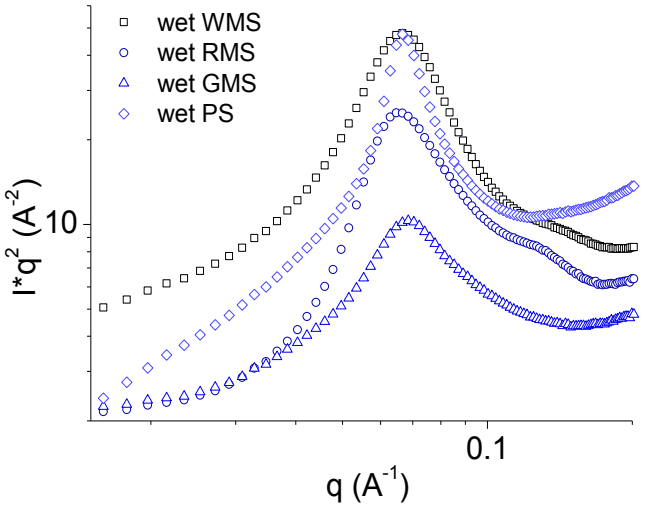

Fig. 2

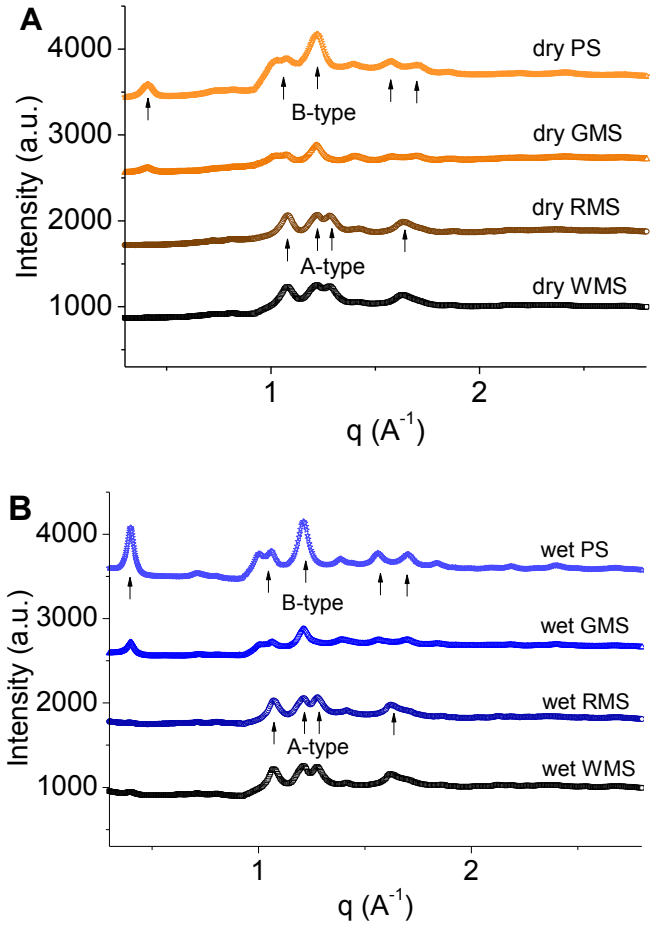

Fig. 3

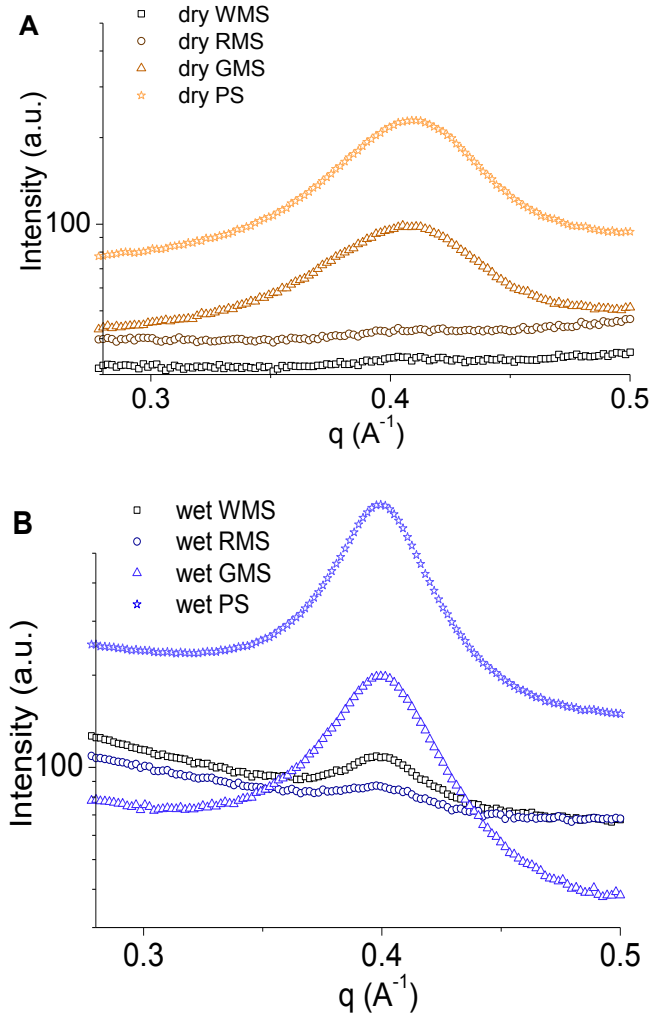

Fig. 4

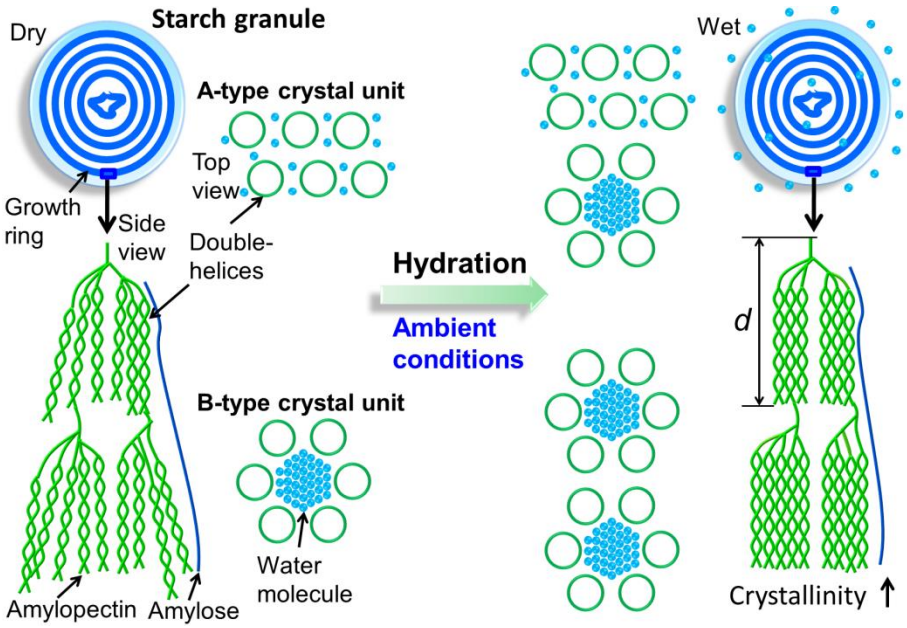

Fig. 5

Table 1 Lamellar peak positions and crystallinity of waxy maize starch (WMS), regular maize starch (RMS), Gelose 50 high amylose maize starch (GMS), and potato starch (PS) before and after hydration under ambient conditions (26 °C) [A]

	Dry				Wet			
	q_{peak1} (Å^{-1})	q_{peak2} (Å^{-1})	X_c (%)	R_{100} (%)	q_{peak1} (Å^{-1})	q_{peak2} (Å^{-1})	X_c (%)	R_{100} (%)
WMS	0.08719±0.00000	--	39.8±1.3	0.02±0.00	0.06281±0.00000	0.1284±0.0000	45.4±0.9	0.43±0.02
RMS	0.07219±0.00000	0.1453±0.0000	38.1±1.0	0.03±0.01	0.06281±0.00000	0.1284±0.0000	44.4±0.8	0.26±0.02
GMS	0.07969±0.00000	--	20.9±0.8	1.80±0.09	0.06469±0.00000	--	22.2±1.2	3.41±0.15
PS	0.07969±0.00000	--	37.2±0.9	2.68±0.10	0.06656±0.00015	--	39.4±1.1	7.57±0.36

[A] q_{peak1} and q_{peak2} are the positions of the lamellar peak and the second order reflection peak, respectively; X_c and R_{100} are the relative crystallinity of starch and the ratio of the area under the 100 inter-helix peak to that under the whole WAXS pattern, respectively.